30

Capillarity Correction to Periodic Solutions of the Shallow Flow Approximation

D. A. Barry, S. J. Barry and J.-Y. Parlange

Abstract

The shallow flow expansion is used to derive equations describing the flow of fluid in an unconfined aquifer. The expansion, which is carried out to second order, is combined with an approximation accounting for the influence of the capillary fringe to give a model that describes the motion of the phreatic surface as it is affected by the capillarity of the porous medium. The results are derived for the case of an aquifer in contact with a reservoir, with the fluid in the reservoir undergoing a steady periodic motion. A linearised solution of the second-order theory is shown to agree well with an "exact" numerical solution. It is demonstrated using the linearised solution that the porous medium capillarity affects the time-averaged mean square height of the phreatic surface of the aquifer in the second-order term, but leaves the first-order term unchanged.

Introduction

Coastal aquifers will respond to the ocean as a result of wave or tidal action, or to variability of recharge. The beach profile also depends on the aquifer configuration. For example, the relative height the water table below the beach affects the amount of erosion of the beach face (e.g., Sato, 1991; Heaton, 1992). In the absence of boundary effects, the evaporative loss of water from the aquifer depends on the depth

Mixing in Estuaries and Coastal Seas
Coastal and Estuarine Studies Volume 50, Pages 496-510

of the water table, which in turn depends on the recharge rate. These effects tend to damp out water table fluctuations. However, near a fluctuating boundary condition such as that imposed by tidal variations, water table movement is dominated by the fluctuations. Previously developed models consider these fluctuations, but do not take into account the effect of the capillary fringe. This effect will be explored below.

Studies of shallow coastal aquifers commonly simplify the governing flow model by invoking the Dupuit assumption of vertical equipotentials in the fluid. The resulting model does not include capillary effects. Therefore, results of such models will be appropriate so long as the capillary fringe length scale is significantly less than any other length scale entering the problem (Parlange *et al.*, 1984). It would appear that this assumption is reasonable in that theoretical predictions and experimental results compare quite well. However, to determine precisely the cause of this result, in this paper we relax the length scale assumption on the capillary fringe. We examine the behaviour of the water level in coastal aquifers (i.e., subject to a periodic boundary condition) utilising a model that includes the effect of the capillary fringe. Note that our purpose is not to model the complex phenomena observed at the zone of interaction (e.g., wave action or sediment transport) between the coastal aquifer and the ocean; rather, it is to quantify directly the effect of the capillary fringe in a physically realistic way. In particular, we focus on the effect of the capillary fringe as it alters the phreatic surface of the aquifer.

The paper is structured as follows: The governing equations modelling the behaviour of the phreatic surface are derived, up to second order, using the shallow flow expansion. Then, an approximation for the time-averaged mean square of true phreatic surface height is presented using the results from the expansion. The second-order theory is then solved, approximately, using a linearisation of the governing equations. An explicit expression for the mean square height is then derived and compared with the analogous case based on the assumption of no capillary fringe.

Derivation of the Governing Equations

We consider isothermal flow of an incompressible fluid in a structurally rigid porous medium. The simplified problem definition is given schematically in Figure 1. The flow domain is assumed to be uniform in the direction normal to the page, i.e., a two-dimensional vertical slice model is analysed. In Figure 1, the ocean is supposed to impose a periodic variation on the boundary of the aquifer, which is located at $x = 0$ (symbol definitions are collected in the notation list). This simplified model isolates the effect of the periodic boundary condition on the free surface of the aquifer, and so mimics the behaviour of a coastal aquifer. The height of the free surface, defined as the position where the fluid pressure is atmospheric, is given by $h(x,t)$. In the region $z > h$, there exists a capillary zone where the fluid pressure is less than

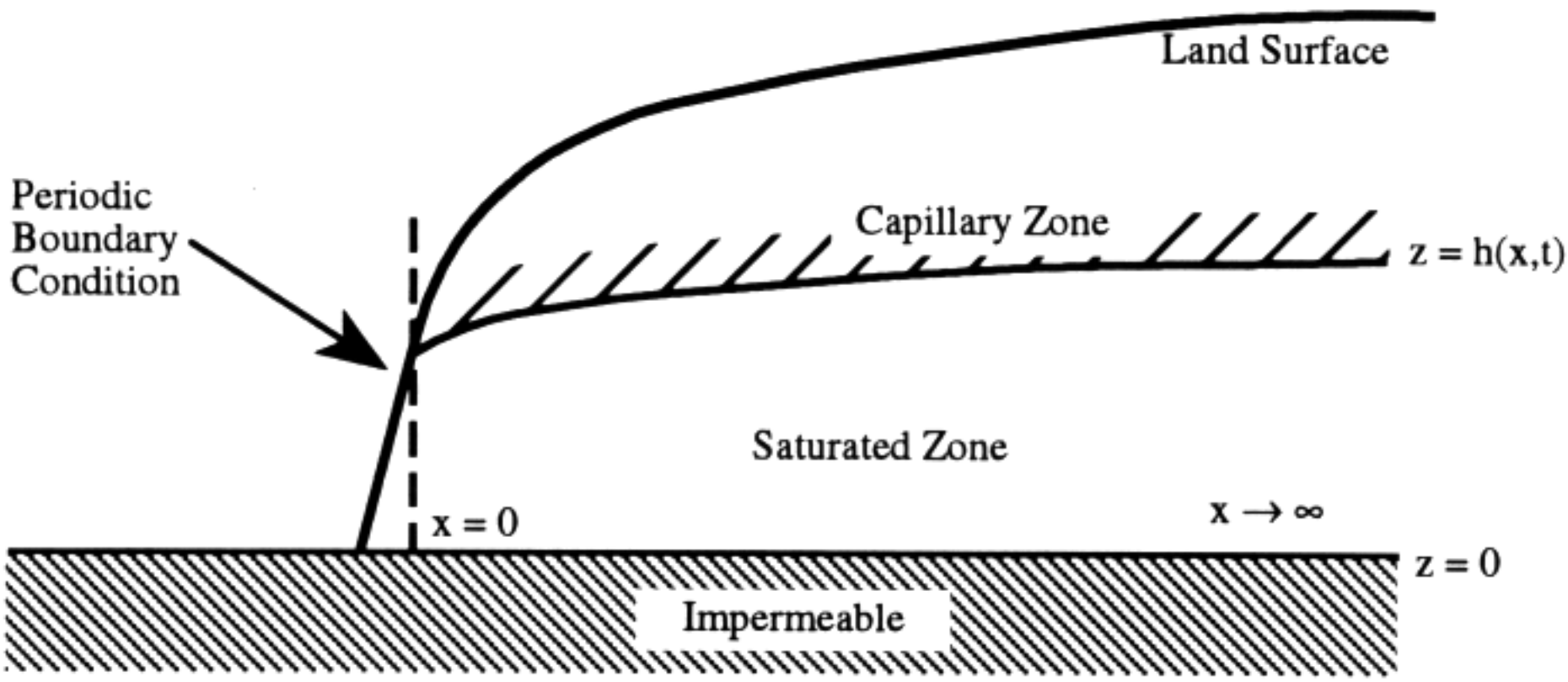

Figure 1. An unconfined aquifer subject to a periodic boundary condition.

atmospheric. The aquifer will be assumed be infinitely long. The fluid potential, ϕ ($= z + p/\rho g$), in the saturated zone then satisfies Laplace's equation since we assume the fluid to be incompressible and the porous medium inelastic (e.g., Bear and Verruijt, 1987), i.e.,

$$\frac{\partial^2 f}{\partial x^2} + \frac{\partial^2 f}{\partial z^2} = 0, \qquad x > 0,\ h > z > 0. \tag{1}$$

A zero-flux condition,

$$\frac{\partial \phi}{\partial z} = 0, \quad z = 0, \tag{2}$$

applies at the impermeable base of the aquifer, while at the phreatic surface we have (e.g., de Marsily, 1986):

$$\phi = h, \qquad z = h, \tag{3}$$

(which simply states that $\psi = 0$ on the phreatic surface), together with the kinematic boundary condition

$$n_e \frac{\partial \phi}{\partial t} = K\left[\left(\frac{\partial \phi}{\partial x}\right)^2 + \left(\frac{\partial \phi}{\partial z}\right)^2\right] + q - (K + q)\frac{\partial \phi}{\partial z}, \qquad z = h. \tag{4}$$

Note that in (1) and (4) we have assumed the hydraulic conductivity, K, in the aquifer to be homogeneous and isotropic. Also, at this point, q is left unspecified although its meaning is clear. It is a source term representing supply of fluid to the free surface from the unsaturated zone. The source could be recharge or, alternatively, supply of capillary fluid.

The Shallow Flow Expansion

In this section we derive an approximation for the free surface height, h, using the shallow flow expansion. The shallow flow expansion was developed by Friedrichs (1948) to derive the shallow water theory. It was subsequently applied by Dagan (1967) to the case of a phreatic aquifer. Following Dagan (1967) (c.f., Bear, 1972) then, (1) to (4) can be expanded using

$$X = x\sqrt{\varepsilon}, \tag{5}$$

$$T = \frac{t\varepsilon K}{n_e}, \tag{6}$$

$$q = K\varepsilon q_1, \tag{7}$$

$$\phi = \phi_0 + \varepsilon\phi_1 + \varepsilon^2\phi_2 + \cdots \tag{8}$$

and

$$h = h_0 + \varepsilon h_1 + \varepsilon^2 h_2 + \cdots, \tag{9}$$

where ε is a perturbation parameter. The precise meaning of the small parameter, ε, in (5)-(9), is unimportant in the expansions because terms of various orders are matched. Nonetheless, the meaning of ε will be discerned below.

The substitution of (5), (6), (8) and (9) into (1) and (2) yields:

$$\phi_0 = c_0(X,T), \tag{10}$$

$$\phi_1 = c_1(X,T) - \frac{z^2}{2}\frac{\partial^2\phi_0}{\partial X^2} \tag{11}$$

and

$$\phi_2 = c_2(X,T) - \frac{z^2}{2}\frac{\partial^2 c_1}{\partial X^2} + \frac{z^4}{24}\frac{\partial^2\phi_0}{\partial X^2}, \tag{12}$$

where c_0, c_1 and c_2 are functions to be determined. To find these functions we first expand (3) and find, on $z = h_0$,

$$\phi_0 = h_0, \tag{13}$$

$$\phi_1 = h_1, \tag{14}$$

and

$$\phi_2 = h_2 + h_0 h_1 \frac{\partial^2 h_0}{\partial X^2}. \tag{15}$$

Equations (13)-(15) can now be used to find the unknown functions in (10)-(12). This operation gives ϕ_0, ϕ_1, and ϕ_2 in terms of h_0, h_1, h_2 and z. Finally, these expressions are used in the expansion of (4), with the following results:

$$\frac{\partial h_0}{\partial T} = \frac{\partial}{\partial X}\left(h_0 \frac{\partial h_0}{\partial X}\right) + q_1 \tag{16}$$

and

$$\frac{\partial h_1}{\partial T} = \frac{\partial^2 (h_0 h_1)}{\partial X^2} + \frac{1}{3}\frac{\partial^2}{\partial X^2}\left(h_0^3 \frac{\partial^2 h_0}{\partial X^2}\right). \tag{17}$$

Equation (16) is the familiar Boussinesq (1903) equation with the source term, q_1. It is interesting to note that q_1 does not enter into the expression (17) defining h_1, and so the latter is identical to the result obtained by Stagnitti *et al.* (1983) and Parlange *et al.* (1984), who ignored capillary effects. In the following, both (16) and (17) are needed to determine an expression for the time-averaged mean-square water table height.

Behaviour of the Time-Averaged Free-Surface Height

As it stands, the model equations are incomplete as boundary conditions have not been imposed. The boundary is assumed to extend vertically upwards from the point x = 0 in Figure 1, on which the periodic condition

$$\phi(0,z,t) = h(0,t) = \gamma\,[1 + \alpha \cos(\omega t)]\,, \tag{18}$$

is applied. On physical grounds we see that $\alpha \leq 1$. We require also that the solution remain bounded as $x \to \infty$, or

$$\frac{\partial \phi}{\partial x} = \frac{\partial h}{\partial x} = 0, \qquad x \to \infty. \tag{19}$$

Drawing on results derived by Knight (1981), Parlange *et al.* (1984) showed that for the periodic boundary condition (18), the time average of h^2, denoted by $\langle h^2 \rangle$, is

$$\langle h^2 \rangle = \langle h_0^2 \rangle + \frac{2}{3}\varepsilon \langle h_0^2 \left(\frac{\partial h_0}{\partial X}\right)^2 \rangle + O(\varepsilon^2), \tag{20}$$

where

$$\langle h_0^2 \rangle = \gamma^2 \left(1 + \frac{\alpha^2}{2}\right). \tag{21}$$

Equation (21) is valid for (16) so long as q_1 has the same period as (18). It shows that the mean square free surface height within the aquifer is always greater than γ^2, although the time-averaged mean height of the forcing at the boundary is γ. This result, which can be derived easily directly from the Boussinesq equation and (18), has the following simple interpretation (Knight, 1981): The effective transmissivity of the aquifer depends on the height of the phreatic surface, so higher water levels on the boundary will result in more water entering the aquifer. The averaged height of water in the aquifer must therefore be greater than that on the boundary so that, on average, the flux at the boundary is zero. Alternatively, it shows that the free surface within the aquifer must be asymmetric. Field data confirm this asymmetry (e.g., Lanyon *et al.*, 1982).

The major contribution of (20) is that $\langle h^2 \rangle$ is determined exactly to $O(\varepsilon)$ by knowledge of h_0 alone, i.e., the solution satisfying (17) for h_1 is not needed. However, although not presented here, (17) was used to obtain (20). For that reason, its derivation (and the consequence that it is independent of q_1) was sketched above. It is common to use (16), or variations of it, to model the behaviour of coastal aquifers (e.g., Nielsen, 1990). Equation (20) shows that estimates of $\langle h^2 \rangle$ based solely on (21) will have an error of $O(\varepsilon)$. In the following this error will be quantified. Before doing so, it is necessary to derive an explicit expression for q_1 that will model the effect of the capillary fringe.

The Capillary Correction

In a recent paper, Parlange and Brutsaert (1987) (cf. Parlange *et al.*, 1990; Fink, 1990) considered the linearised version of (16) and derived an estimate of q_1 based on that linearisation. If (16) is taken as the point of departure, it is possible to use the approach of Parlange and Brutsaert (1987) to derive (in dimensional form)

$$n_e \frac{\partial h_0}{\partial t} = K \frac{\partial}{\partial x}\left(h_0 \frac{\partial h_0}{\partial x}\right) + B \frac{\partial^2}{\partial t \partial x}\left(h_0 \frac{\partial h_0}{\partial x}\right), \tag{22}$$

where B is approximated by

$$B \simeq \int_{-\infty}^{0} \theta - \theta_r \, d\psi. \tag{23}$$

Thus, B represents, for example, the average depth of water held in the capillary zone above the phreatic surface, or the average suction required to remove the capillary water from the unsaturated zone.

Equation (22) is a nonlinear model that incorporates the effect of capillarity on h_0. Observe that because the final term on the right-hand side of (22) is periodic if h_0 is periodic, the time average given in (21) remains unchanged by capillarity, as might be expected. Clearly, however, capillarity will influence the first-order term on the right-hand side of (20).

In order to estimate $\langle h^2 \rangle$ in (20), we must solve (22) subject to the following conditions resulting from (18) and (19):

$$h_0(0,t) = \gamma [1 + \alpha \cos(\omega t)] \tag{24}$$

and

$$\frac{\partial h_0}{\partial x} = 0, \qquad x \to \infty. \tag{25}$$

Equations (24) and (25) are the boundary conditions which the solution to (22) must satisfy. Clearly, an initial condition is needed to complete the specification of the problem, and any initial condition could be invoked. As time progresses, however, "memory" of the initial condition will be lost and, eventually, a quasi-steady state will be attained. Regardless of the initial condition, the behaviour of the system will be influenced wholly by the boundary condition (24). Therefore, in what follows we look for the periodic solution only, i.e., the solution that applies after a long time when all transient effects due to the initial condition have decayed.

Estimation of h_0

The solution of (22)-(25) is required to determine $\langle h^2 \rangle$ in (20). In general, such a solution will be obtained numerically. However, the numerical solution will not give ε. This parameter can be determined from an analytical solution satisfying (22)-(25). In this section an approximate analytical solution is calculated.

Motivated by the boundary condition (24), we seek an approximate solution in the form;

$$h_0(x,t) = \gamma [1 + \alpha h_{0,1}(x,t) + \alpha^2 h_{0,2}(x,t) + \dots], \tag{26}$$

i.e., α is treated as a perturbation parameter. Clearly, (26) will be accurate for $\alpha << 1$. Upon substituting (26) into (22)-(25) we find that the $O(\alpha)$ terms give the following problem defining $h_{0,1}$:

$$n_e \frac{\partial h_{0,1}}{\partial t} = K\gamma \frac{\partial^2 h_{0,1}}{\partial x^2} + B\gamma \frac{\partial^3 h_{0,1}}{\partial t \partial x^2}, \tag{27}$$

$$h_{0,1}(0,t) = \cos(\omega t) \tag{28}$$

and

$$\frac{\partial h_{0,1}}{\partial x} = 0, \qquad x \to \infty. \tag{29}$$

Equations (27)-(29) have the obvious solution:

$$h_{0,1} = \exp(-x\lambda P)\cos(\omega t - x\lambda Q), \tag{30}$$

where

$$\lambda = \sqrt{\frac{n_e \omega}{2K\gamma}}, \tag{31}$$

$$\begin{bmatrix} P \\ Q \end{bmatrix} = \sqrt{\frac{1}{\sqrt{1+\omega^{*2}}} \begin{bmatrix} + \\ - \end{bmatrix} \frac{\omega^*}{1+\omega^{*2}}} \tag{32}$$

and

$$\omega^* = \frac{\omega B}{K}. \tag{33}$$

Stagnitti *et al.* (1983) point out that the problem defined by (27)-(29) was solved by Steggewentz (1933) for the case of no capillary term, i.e., B = 0. Setting B = 0 in (30) yields

$$h_{0,1}\big|_{B=0} = \exp(-x\lambda)\cos(\omega t - x\lambda). \tag{34}$$

Equation (34) agrees with the corresponding result reported by Lewandowski and Zeidler (1978), Parlange *et al.* (1984) and Nielsen (1990).

We proceed now to the calculation of $h_{0,2}$. The $O(\alpha^2)$ expressions resulting from the use of (26) in (22)-(25) are

$$n_e \frac{\partial h_{0,2}}{\partial t} = K\gamma \frac{\partial^2 h_{0,2}}{\partial x^2} + B\gamma \frac{\partial^3 h_{0,2}}{\partial t \partial x^2} + \frac{\gamma}{2}\left(K + B\frac{\partial}{\partial t}\right)\frac{\partial^2 h_{0,1}^2}{\partial x^2}, \tag{35}$$

$$h_{0,2}(0,t) = 0 \tag{36}$$

and

$$\frac{\partial h_{0,2}}{\partial x} = 0, \qquad x \to \infty. \tag{37}$$

The solution for $h_{0,2}$ satisfying (35)-(37) can be shown to be:

$$h_{0,2} = \frac{1}{4}\left[1 - \exp(-2x\lambda P)\right] + \frac{1 + 6\omega^{*2}}{2\left(1 + 9\omega^{*2}\right)}\left[\exp(-\sqrt{2}x\lambda P_1)\cos(\beta_1) - \exp(-2x\lambda P)\cos(\beta)\right]$$
$$+ \frac{\omega^{*}}{2\left(1 + 9\omega^{*2}\right)}\left[\exp(-\sqrt{2}x\lambda P_1)\sin(\beta_1) - \exp(-2x\lambda P)\sin(\beta)\right], \tag{38}$$

where

$$\begin{bmatrix} P_1 \\ Q_1 \end{bmatrix} = \sqrt{\frac{1}{\sqrt{1 + 4\omega^{*2}}}\begin{bmatrix} + \\ - \end{bmatrix}\frac{2\omega^{*}}{1 + 4\omega^{*2}}}, \tag{39}$$

$$\beta = 2\omega t - 2x\lambda Q \tag{40}$$

and

$$\beta_1 = 2\omega t - \sqrt{2}x\lambda Q_1. \tag{41}$$

Setting B = 0 in (39) yields

$$h_{0,2}\Big|_{B=0} = \frac{1}{4} - \frac{\exp(-2x\lambda)}{4} + \frac{1}{2}\left[\exp(-\sqrt{2}x\lambda)\cos(2\omega t - \sqrt{2}x\lambda) - \exp(-2x\lambda)\cos(2\omega t - 2x\lambda)\right], \tag{24}$$

in agreement, again, with the results reported by Parlange *et al.* (1984) and Nielsen (1990). Note that, by comparison with (34) and (42), (30) and (38) indeed represent a correction to the standard Boussinesq solution, i.e., the same basic form is obtained except that the various parameters become functions of ω^*.

With $h_{0,1}$ and $h_{0,2}$ now evaluated in (30) and (38), respectively, (26) can be used to evaluate h_0 analytically. This expression will be used shortly to determine ε in (20). Before doing so, however, the validity of (26) as an approximation for h_0 needs to be evaluated. For this purpose a numerical solution for (22)-(25) was developed. The details of this numerical solution are presented in the Appendix.

The "exact" numerical solution and the analytical approximation, (26), are compared in Figure 2. Because the approximation is exact for $\alpha = 0$, we took the extreme value of $\alpha = 1$ in order to check (26). Note that checking $\alpha = -1$ is unnecessary since it changes only the phase of the boundary condition (24).

Because the initial condition is unimportant, $h_0(x,0)$, calculated using (26), was used as the initial condition for the numerical solution. The results in Figure 2 show that the analytical approximation is satisfactory, even for this extreme case.

These results suggest further that (26) is suitable for estimating $\langle h^2 \rangle$ in (20). Using the expansion for h_0 in (26) gives

$$\frac{\langle h^2 \rangle}{\gamma^2} = \frac{\langle h_0^2 \rangle}{\gamma^2} + \frac{\alpha^2 n_e \gamma \omega \exp(-2x\lambda P)}{3K\left(1+\omega^{*2}\right)}. \tag{43}$$

For $B = 0$ ($\omega^* = 0$, $P = 1$), (43) reduces to the analogous expression reported by Parlange *et al.* (1984). In addition, (43) indicates that the perturbation parameter, ε, is given by (using dimensional quantities)

$$\varepsilon = \frac{\alpha^2 n_e \gamma \omega K}{6\left(K^2 + B^2\omega^2\right)}. \tag{44}$$

Equation (44) contains an interesting result, not reported previously. It predicts that the coefficient of the exponential in the second-order term of (43) will be maximised for a particular value of ω ($\approx K/B$). Thus, the second-order term is a maximum for this value of ω at $x = 0$.

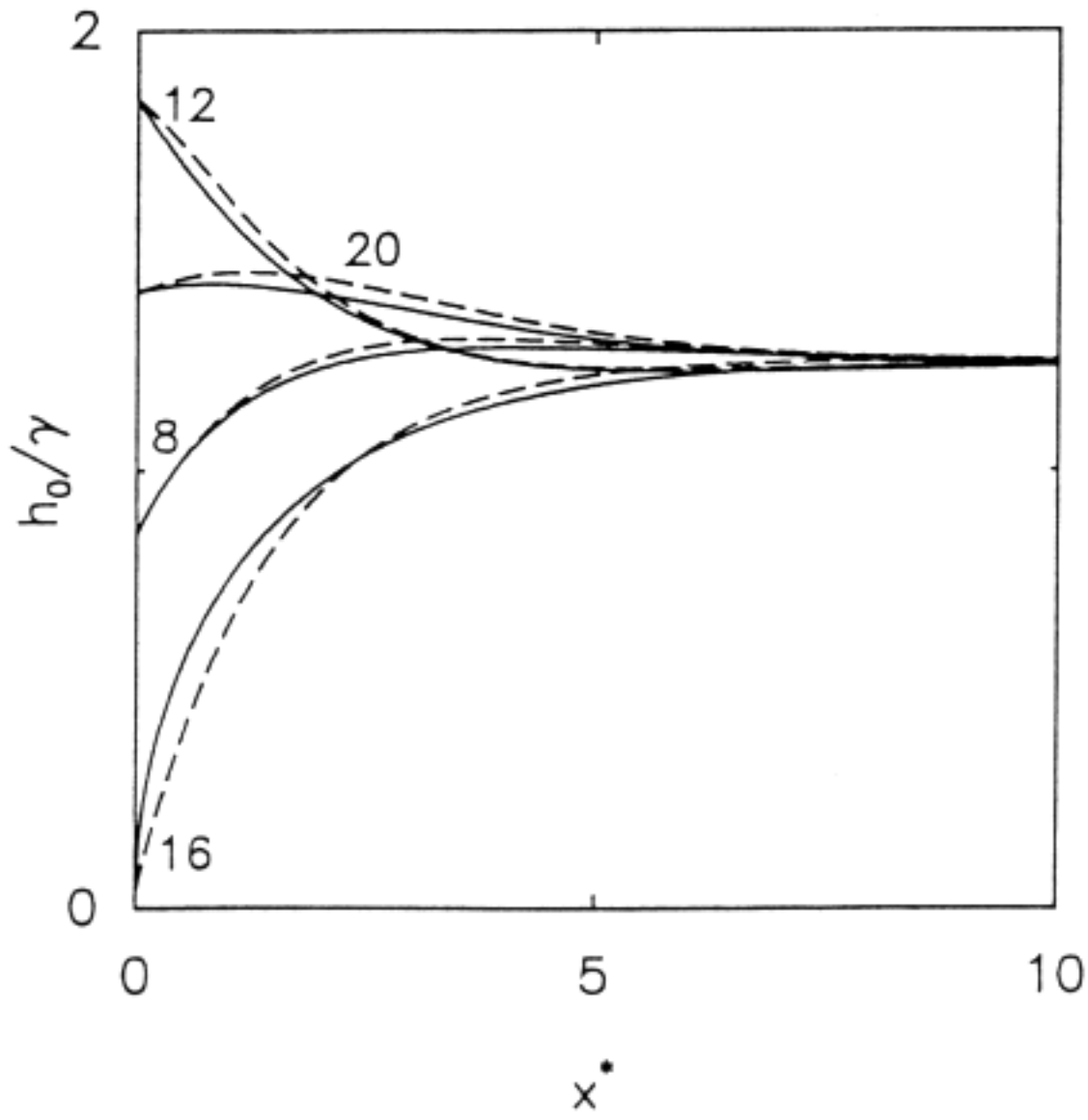

Figure 2. Comparison of "exact" numerical solution (Appendix) - lines - satisfying (22)-(25) and the analytical approximation (26) - dashes - for $\alpha = 1$ and $\omega^* = 1$. Labels on the curves give values of t^*.

Discussion and Conclusions

The main result of this study is contained in (43), which gives the time-averaged mean square height of the free surface in the aquifer. Only a few reports of appropriate laboratory experiments are available in the literature, and these are usually analysed using the Boussinesq equation, i.e., (22) with B = 0. For this reason the experiments were carried out using porous media composed of coarse materials so that the capillary effect on the free surface would be minimised. For example, Smiles and Stokes (1976) used a Hele-Shaw model while Parlange *et al.* (1984) used 0.5 cm diameter gravel. It is, therefore, not surprising that Parlange *et al.* (1984), who neglected capillary effects in their analysis, found that the experimental results were predicted quite well. Clearly, neither of these data sets can usefully be analysed using (43). Thus, at present we cannot provide experimental evidence to confirm our results. This is unfortunate because, paradoxically, the theory predicts that the correction term in (43) reduces in magnitude as B increases, and so the first term, $\langle h_0^2 \rangle$, dominates. It is clear physically why this is so: Due to capillarity, water can be stored in the unsaturated zone and it becomes easier for the groundwater to follow the fluctuations imposed at x = 0.

It is possible to show, approximately, the effect of the capillarity correction by inserting typical parameter values in (43). To simplify matters we set x = 0. Then, the only place where non zero values of the capillarity parameter, B, enter is in the denominator of the final term, through ω^*. If $\omega^* \ll 1$, then capillarity has negligible influence. Typical parameter values for a sandy beach with ocean tidal forcing are (e.g., Bear and Verruijt, 1987) K = 10 m d^{-1}, ω = 2 d^{-1} and B = 0.5 m, yielding ω^* = 0.1. On the other hand, parameters relevant for a lake undergoing seasonal variations in its water level that is connected with a relatively low permeability aquifer might be ω = 2 yr^{-1}, K = 0.01 m d^{-1}, B = 2 m, giving $\omega^* \approx 1.1$. This range of values suggests, not surprisingly, that the capillarity effect is important only in relatively low conductivity, small grained media.

Equation (43) also shows that the decay length of the fluctuations in the porous medium due to the fluctuating water body is of order $l_f = 2(\lambda P)^{-1}$. For a coastal aquifer, we take as the depth of the aquifer, γ, the magnitude of the tidal fluctuation, since the fresh water aquifer is underlain by the salt wedge which, for the purpose of an order of magnitude calculation, may be taken as being stationary. To compute λ we take the values used above with n_e = 0.35 and γ = 1.7 m. Thus, tidal fluctuations on a sandy beach are approximately l_f = 13.3 m, with B = 0.5 m or 13.9 m with no capillary effect, B = 0. If, on the other hand, γ is taken as the entire depth of the aquifer, say 15 m, then l_f = 39.6 m, with B = 0.5 m or 41.4 m with B = 0. The actual range probably lies between these limits. Some data on beach water table fluctuations at a Wollongong (New South Wales, Australia) beach is available from the study of Lanyon *et al.* (1982, Table 4). A 1.7 m tidal range decays to 0.15 of this value over a distance of 23 m. Similar calculations can be performed for the lake example discussed above. The same parameter values are used along with n_e = 0.45 and γ = 15 m yielding l_f = 20.4 m or 22.1 m with B = 0. These representative cases

show that the decay length of the fluctuations at the boundary are little affected by capillarity.

Finally, these results suggest that, because the effect of capillarity is relatively small, the Boussinesq solution (neglecting capillarity) will be good in situations where the parameters are curve fitted with ad hoc parameters.

References

Barry, D.A., Parlange, J.-Y., and Starr, J.L. Numerical analysis of the precursor effect, *Soil Sci.*, 143, 309-317, 1987.

Barry, D.A., Starr, J.L., Parlange, J.-Y., and Braddock, R.D. Numerical analysis of the snow-plow effect, *Soil Sci. Soc. Am. J.*, 47, 862-868, 1983.

Bear, J. *Dynamics of fluids in porous media*, American Elsevier, New York, 1972.

Bear, J., and Verruijt, A. *Modeling groundwater flow and pollution*, D. Reidel, Dordrecht, 1987.

Boussinesq, J. Recherches theoretiques sur l'ecoulemant des nappes d'eau infiltrées dans le sols et sur debit de sources, *C. R. Hebd. Seances Acad. Sci.*, 10, 7-78, 1903.

Crank, J., and Nicolson, P. A practical method for numerical evaluation of solutions of equations of the heat-conduction type, *Proc. Camb. Philos. Soc.*, 43, 50-67, 1947.

Dagan, G. Second-order theory of shallow free-surface flow in porous media, *Q. J. Mech. Appl. Math.*, 20, 517-526, 1967.

de Marsily, G. *Quantitative hydrogeology*, Academic Press, San Diego, 1986.

Fink, J.P. Curious behavior of a groundwater flow model. *Water Resour. Res.*, 26, 1833-1836, 1990.

Friedrichs, K.O. On the derivation of the shallow water theory (Appendix to a paper by J. J. Stoker), *Comm. Appl. Math.*, 1, 81-85.

Heaton, K. Local effects of groundwater table variations on on-shore off-shore sediment transport. Honours thesis, Dept Civil & Environ. Eng., Univer. West. Aust., 1992.

Knight, J.H. Steady periodic flow through a rectangular dam, *Water Resour. Res.*, 17, 1222-1224, 1981.

Lanyon, J.A., Elliot, I.G., and Clarke, D.J. Groundwater-level variation during semidiurnal spring tidal cycles on a sandy beach, *Aust. J. Mar. Freshwater Res.*, 33, 377-400, 1982.

Lewandowski, A., and Zeidler, R.B. Beach ground-water oscillations, *Proc. 16th Coastal Eng. Conf.*, Am. Soc. Civ. Eng., New York, II, 2051-2065, 1978.

Nielsen, P. Tidal dynamics of the water table in beaches. *Water Resour. Res.*, 26, 2127-2134, 1990.

Parlange, J.-Y., and Brutsaert, W. A capillary correction for free surface flow of groundwater, *Water Resour. Res.*, 23, 805-808, 1987.

Parlange, J.-Y., Brutsaert, W., Fink, J.P., and El-Kadi, A.I. A capillary correction for free surface flow revisited, *Water Resour. Res.*, 26, 1691-1692, 1990.

Parlange, J.-Y., Stagnitti, F., Starr, J.L., and Braddock, R.D., Free-surface flow in porous media and periodic solution of the shallow-flow approximation, *J. Hydrol.*, 70, 251-263, 1984.

Sato, M. Underground water table and beach face erosion, in B. L. Edge (ed.), *Proc. 22nd Coastal Eng. Intl. Conf.*, Am. Soc. Civil Eng., New York, 2644-2657, 1991.

Stagnitti, F., Parlange, J.-Y., Starr, J.L., Chu, B.T., and Braddock, R.D. Water level variations in aquifers caused by ocean tides, *Proc. 6th Aust. Conf. on Coastal & Ocean Eng.*, Gold Coast, Qld. 13-15 July, 216-219, 1983.

Steggewentz, J.H. De invloed van de getijbeweging van zeeen en getijrivieren op de stijghoogte van het groundwater. Thesis, Delft University of Technology, Holland, 1933.

Thomas, L.H., Elliptic problems in linear difference equations over a network, Watson Scientific Computing Lab., Columbia Univ., New York, NY, 1949.

Appendix

A numerical solution satisfying (22), (24), (25) and an arbitrary initial condition is developed here. If we define the dimensionless free surface height, h^*, as

$$h^* = h/\gamma \tag{A1}$$

then, in dimensionless form, the problem to be solved is

$$\frac{\partial h^*}{\partial t^*} = \frac{\partial^2 h^{*2}}{\partial x^{*2}} + \frac{\partial^3 h^{*2}}{\partial t^* \partial x^{*2}} \tag{A2}$$

subject to

$$h^*(0,t^*) = 1 + \alpha \cos\left(\omega^* t^*\right), \tag{A3}$$

$$\frac{\partial h^*}{\partial x^*} = 0, \qquad x^* \to \infty \tag{A4}$$

and

$$h^*(x^*,0) = h^*_{in}(x^*). \tag{A5}$$

In the numerical solution, (A4) is applied at a finite distance, with that distance chosen so that the effect of the finite domain size is negligible. Equations (A2)-(A5) are now transformed using the substitution $u = h^{*2}$. The resulting equations are then solved using the approach of Crank and Nicolson (1947), i.e., we take centred finite difference approximations to both the spatial and temporal derivatives about the point $[j\Delta x^*, (n + 1/2)\Delta t^*]$, where $x^* = j\Delta x^*$, $j = 0, ..., N$ and $t^* = n\Delta t^*$, $n = 0, ..., M$. The method yields the following system of equations to be solved

$$\mathbf{A}(r)^{n+1}\mathbf{u}^{n+1} = \mathbf{A}(s)^{n}\mathbf{u}^{n} + \mathbf{b}, \tag{A6}$$

where

$$\mathbf{u}^n = \left[u_1^n, u_2^n, \ldots, u_{N-1}^n, u_N^n\right]^T, \tag{A7}$$

$$\mathbf{A}(s)^n = \begin{bmatrix} D_1 & -s & 0 & \cdots & & 0 \\ -s & D_2 & -s & 0 & & \\ 0 & \ddots & \ddots & \ddots & & \vdots \\ \vdots & & \ddots & \ddots & \ddots & \\ & \cdots & 0 & -s & D_{N-1} & -s \\ 0 & & \cdots & 0 & -2s & D_N \end{bmatrix}, \tag{A8}$$

$$\mathbf{b} = \left[\left\{1 + \alpha \cos\left(j\omega^* \Delta t^*\right)\right\}^2 s + \left\{1 + \alpha \cos\left((j+1)\omega^* \Delta t^*\right)\right\}^2 r, 0, \cdots, 0\right]^T \quad \text{(A9)}$$

$$\begin{bmatrix} r \\ s \end{bmatrix} = \frac{1}{\Delta x^{*2}} \left(\frac{\Delta t^*}{2} \begin{bmatrix} + \\ - \end{bmatrix} 1 \right). \quad \text{(A10)}$$

and

$$D_i = 2s + \frac{1}{\sqrt{u_i^n}}, i = 1, \ldots, N \quad \text{(A11)}$$

Equation (A6) defines a nonlinear system of equations to be solved on successive time lines, j, j + 1, etc., with the j = 0 time line determined from the initial condition (A5). Fixed-point iteration was used to solve (A6) at each time line, i.e., the coefficient matrix $\mathbf{A}^{j+1}$ was linearised by setting the unknown terms on the diagonal to the values computed at the previous time step. The resulting linear system was then solved using the efficient Thomas (1949) algorithm. The updated estimates contained in **u** were substituted into $\mathbf{A}^{j+1}$ and the procedure repeated until convergence (defined as when each element in successive estimates of **u** differed by less than 10^{-12}). The calculations then proceeded to the next time step.

A consistency analysis shows this scheme has an error term of $O(\Delta x^{*2}, \Delta t^{*2})$. The scheme is similar to those used by Barry *et al.* (1983, 1987), where further details of its properties can be found.

Notations

A	coefficient matrix in the finite-difference solution (Appendix)
b	forcing term in finite-difference solution (Appendix)
B	coefficient in capillary correction term, L
c_i	i = 0, 1, 2, arbitrary functions, L
D_i	i=1, ..., N, defined by (A11)
g	magnitude of gravitational acceleration, LT^{-2}
h	height of the free surface, L
h^*	dimensionless free surface height, (A1)
h^*_{in}	arbitrary function of x^*, (A5)
h_i	i = 1, 2, ..., functions appearing in the expansion of h, L
$h_{0,i}$	i = 1, 2, ..., functions appearing in the expansion of h_0
j	spatial counter used in the finite-difference solution (Appendix)
K	hydraulic conductivity, LT^{-1}
l_f	fluctuation length scale, L
M	maximum number of temporal steps in the finite-difference grid (Appendix)

n	temporal counter used in the finite-difference solution (Appendix)
n_e	effective porosity
N	maximum number of spatial steps in the finite-difference grid (Appendix)
p	fluid pressure offset such that p = 0 is atmospheric pressure, $ML^{-1}T^{-2}$
P	function of ω^*, (32)
P_1	function of ω^*, (39)
q	flux of fluid supplied to the saturated zone, LT^{-1}
q_1	flux of fluid supplied to the saturated zone (dimensionless form)
Q	function of ω^*, (32)
Q_1	function of ω^*, (39)
r	factor used in finite-difference solution (Appendix)
s	factor used in finite-difference solution (Appendix)
t	time, T
t^*	tK/B, dimensionless time variable
T	scaled time, L
u	function of h^* (Appendix)
u	vector used in finite-difference solution (Appendix)
x	distance from the location of the forcing boundary condition, L
x^*	$x\sqrt{\frac{2n_e}{B\gamma}}$, dimensionless position variable
X	scaled position, L
z	distance above the impermeable base of the aquifer, L
α	the semi-tidal amplitude (maximum possible relative fluid fluctuation at x = 0)
γ	mean water depth at x = 0, L
Δx^*	spatial grid size used in the finite-difference solution
Δt^*	temporal grid size used in the finite-difference solution
ε	perturbation parameter
θ	volumetric moisture content
θ_r	residual volumetric moisture content
ρ	fluid density, ML^{-3}
ϕ	$z + \psi$, piezometric head, L
ϕ_i	i = 1, 2, ..., functions appearing in the expansion of ϕ, L
ψ	pressure head, $p/\rho g$, L
ω	frequency, T^{-1}
ω^*	dimensionless frequency, (33)
$\cdot^T$	transpose of $\cdot$
$\langle\cdot\rangle$	time average of $\cdot$